

Structural Analysis of Cadmium–Glycylglycine Complexes Studied by X-Ray Diffraction and High Resolution ^{113}Cd and ^{13}C Solid State NMR

Toshio Takayama,* Shirabe Ohuchida, Yoshio Koike, Masanobu Watanabe,
Daisuke Hashizume,† and Yuji Ohashi†

Department of Applied Chemistry, Faculty of Engineering, Kanagawa University, Rokkakubashi, Yokohama 221

†Department of Chemistry, Faculty of Science, Tokyo Institute of Technology, O-okayama, Meguro-ku, Tokyo 152

(Received January 11, 1996)

Structural analysis of bis(glycylglycinato)cadmium(II) complexes prepared to adjust the pH to 6 (**A**) and 9 (**C**), were studied by X-ray diffraction and high resolution ^{113}Cd and ^{13}C solid state NMR. In order to compare with the structure of **A**, structural analysis of bis(glycylglycinato)zinc(II) complexes (**B**) prepared to adjust the pH to 6 was also performed by the same methods. The structure of **A** was six coordinate; a five-membered chelate ring was formed between the terminal amino-group and the adjacent O (peptide) and the terminal carboxygroups of the dipeptide ligands were involved in Cd binding in the complex. The structure of **B** was similar to **A**, indicating that the Cd nucleus was better suited for probing the Zn nucleus-ligand structure. The structure of **C** was six coordinate; the four terminal carboxygroups (O) and the two terminal aminogroups (N) of the dipeptide ligands were involved in Cd binding in the complex. High-resolution ^{113}Cd and ^{13}C CP/MAS NMR spectra have been measured in order to obtain detailed information about the structures. The ^{113}Cd signal of **A** showed a low field chemical shift compared with the peak of **C**. This means that the chelate ring shows decreased shielding. From the ^{13}C spectra of **A** and **C**, it was seen that the Cd nucleus of **A** is bonded to a carbonyl oxygen (peptide) and the terminal carboxyl group of the dipeptide, but that for **C** is not bonded to a carbonyl oxygen (peptide).

The role of several trace metals in living organisms has been designated as either structure-promotion or enzyme activation/deactivation. For elements such as zinc, cadmium, and mercury, general complexation studies are important in obtaining a more fundamental understanding of biochemical systems.¹⁾ The first of these properties is attributed to an increase in the susceptibility of the peptide linkage to hydrolysis, owing to binding of the C-terminal group of the peptide to the zinc atom at the active site of the enzyme. Replacement of zinc by cadmium results in partial loss of the catalytic activity for cleavage of the C-terminal amino acid residue, but the modified enzymes still catalyse the hydrolysis of esters.²⁾

Our knowledge of the solubility products of metallic hydroxides is not very precise, so that it is not always possible to make exact theoretical calculations. The precipitation will depend largely upon the solubility product ($\text{Cd}(\text{OH})_2 : K_{\text{sp}} 2.5 \times 10^{-14}$) of the metallic hydroxide and the hydroxide-ion concentration. The approximate calculated pH value at which the hydroxide begins to precipitate from 0.01 mol dm⁻³ cadmium solution is 8.2.

When glycylglycine is dissolved in water, the various hydrogen atoms undergo ionization to different extents. The primary and secondary dissociation constants are $\text{p}K_1^{\text{H}} = 3.18$ and $\text{p}K_2^{\text{H}} = 8.15$ ($I = 0.1$, NaClO_4 ; 25 °C).³⁾

For the coordination of cadmium ion to glycylglycine by the addition of hydroxide, the following possibilities have

been taken into account.⁴⁾ The carboxyl and amino groups are protonated at $\text{pH} < 3$ and as the pH is increased from 3 to 8, it is considered likely that the terminal carboxyl and terminal amino groups are simultaneously coordinated to the same cadmium ion, and the peptide linkage adjacent to the terminal amino group might also be simultaneously coordinated through the carbonyl oxygen atom resulting in a five-membered chelate ring. Further, coordination of the terminal amine of a carboxylate-coordinated peptide group to another cadmium ion and coordination of a carboxylate-coordinated cadmium ion to the terminal amine of another glycylglycine could presumably take place. At $\text{pH} > 8.2$, coordination of hydroxide by the cadmium ion may also occur, particularly at the highest pH attainable. However the presence of such coordination could rarely be detected, because the complexation of cadmium ion and glycylglycine preferentially occurs before the beginning of precipitation of cadmium hydroxide.

NMR studies with cadmium as the probe ion have been used to elucidate the nature of metal binding in zinc-activated metalloenzymes.^{5–8)} The ^{113}Cd nucleus, with its chemical shift range of over 600 ppm, gives NMR sensitivity five times that of the ^{13}C nucleus and thus is better suited for probing metal-ligand interactions.⁹⁾ Combined ^{113}Cd and ^{13}C NMR studies of a homologous series of cadmium-amino acid complexes have already been reported,¹⁰⁾ and are

interpreted as suggesting that five-membered chelate rings form between cadmium and amino acids. The Cd-nucleus chemical shift has been demonstrated to be a sensitive probe for solvent effects and complexation studies. However, a serious limitation to this approach has been the lack of correlation between a reliable structure and the shift to use as the basis of interpreting measured Cd-nucleus chemical shifts. This kind of approach is often unwarranted in metal-nuclide work, because of the lability and/or uncertainties in metal ion coordination in the system.

This problem has been solved in the following manner. The most stable structures of the Cd-complexes formed with the zwitterionic form (pH=6) and the anionic form at pH=9 of glycylglycine could be well confirmed by precipitation from the solutions.

An approach that we have adopted is to determine the chemical shifts of the Cd nucleus in structurally characterized solids for interpreting the chemical shifts of solutions. As the nature of the coordination in these structurally characterized solid species¹¹⁾ (e.g., species studied by X-ray diffraction) is established, the empirical relationships between chemical shifts of the Cd nucleus and coordination details can therefore be established directly.

Recently developed techniques for high-resolution NMR spectroscopy of solids^{12–14)} now provide the opportunity to study the chemical shift of the Cd nucleus in well-defined crystalline environments. The sensitivity of the ¹¹³Cd resonance has been greatly improved by introduction of cross-polarization magic angle spinning (CP/MAS) methods.^{15–18)} However, few attempts have yet been made to relate the ¹¹³Cd chemical shifts for cadmium-binding peptides in the solid state.

The resonance obtained in this way can be roughly comparable to what would be obtained in solution, if the crystalline environment could be preserved intact in the mobile molecular regime of the liquid state. Some of these current studies make use of the ¹¹³Cd nucleus as a probe of the structures of metalloproteins, with Cd(II) occurring in the natural protein or as a substitute for some other metal ion, e.g., Zn(II).

This paper presents structural analyses of compounds for metalloprotein, bis(glycylglycinato)cadmium(II) complexes prepared to adjust the pH to 6 and 9, studied by X-ray diffraction and high resolution ¹¹³Cd and ¹³C solid state NMR. In order to compare with the structure of the Cd complex at pH 6, structural analysis of a bis(glycylglycinato)zinc(II) complex, prepared to adjust the pH to 6, was also performed by the same methods.

Experimental

Syntheses. (A) [Cd(glycylglycine)₂] \cdot 2H₂O pH=6: [Cd(glygly)₂ \cdot 2H₂O pH=6]; (B) [Zn(glygly)₂] \cdot 2H₂O pH=6; and (C) [Cd(glygly)₂] \cdot H₂O pH=9 were prepared by the following method. A was formed to adjust the pH to 6 in a water solution (100 ml) containing Cd(NO₃)₂ \cdot 4H₂O (3.08 g, 10 mM, 1 M=1 mol dm⁻³) and glycylglycine (2.64 g, 20 mmol dm⁻³); B was obtained by adjusting the pH to 6 in a water solution (100 ml) containing Zn(NO₃)₂ \cdot 6H₂O (2.97 g, 10 mmol dm⁻³) and glycylglycine (2.64 g, 20 mmol dm⁻³);

and C was obtained by adjusting the pH to 9 with sufficient NaOH in a water solution (100 ml) containing Cd(NO₃)₂ \cdot 4H₂O (3.08 g, 10 mM) and glycylglycine (2.64 g, 20 mmol dm⁻³). Complexes A—C were crystallized by slow evaporation. A: Yield 0.51 g (12.9%). Found: C, 23.27; H, 4.35; N, 13.61%. Calcd for Cd(glygly)₂ \cdot 2H₂O: C, 23.34; H, 4.40; N, 13.62%. B: Yield 1.07 g (29.5%). Found: C, 26.44; H, 5.09; N, 15.37%. Calcd for Zn(glygly)₂ \cdot 2H₂O: C, 26.42; H, 4.99; N, 15.41%. C: Yield 1.69 g (43.0%). Found: C, 23.94; H, 13.91; N, 4.20%. Calcd for Cd(glygly)₂ \cdot H₂O: C, 24.47; H, 14.27; N, 4.11%.

NMR Measurements. ¹¹³Cd CP/MAS NMR spectra were recorded on a JEOL EX-270 NMR spectrometer operating at 59.79 MHz with a CP/MAS accessory. Samples (ca. 100 mg) containing the naturally abundant ¹¹³Cd nuclide were contained in a cylindrical rotor made of zirconia and spun at a speed of up to 5.8–6.2 kHz. Contact time was 5 ms, and repetition time was 5 s. The spectral width and data points were 185.2 kHz and 8 kHz, respectively. Spectra were usually accumulated 400–2000 times to achieve a reasonable signal-to-noise ratio at room temperature. Spectra consisting of a series of peaks separated by the spinning frequency (spinning side band) are cases of “slow spinning”, in which the MAS frequency is considerably less than the shift anisotropy. The peak that is independent of the spinning frequency corresponds to the isotropic chemical shift. The ¹¹³Cd NMR chemical shifts were calibrated indirectly through external solid Cd(NO₃)₂ \cdot 4H₂O and converted to Cd(ClO₄)₂ \cdot 6H₂O (δ =0.0). ¹³C CP/MAS NMR spectra were measured by a conventional method and the chemical shifts were converted to tetramethylsilane (TMS) (δ =0.0).

X-Ray Crystal Structure Analysis. The crystal data and experimental details are summarized in Table 1.

Lorentz, polarization, and absorption corrections were applied to all crystals, and the extinction correction was applied only to A. The structures of B and C were solved by the direct method with the program SIR-92.¹⁹⁾ The final structure of B was used as an initial structure for A. All the structures were refined by the full-matrix least-squares method with the program SHELXL-93.²⁰⁾ The weighting schemes were $w=[\sigma(F_o^2)^2+(0.0340P)^2+0.5909P]^{-1}$, $w=[\sigma(F_o^2)^2+(0.0416P)^2+0.3142P]^{-1}$, and $w=[\sigma(F_o^2)^2+(0.0411P)^2+0.2988P]^{-1}$ for A, B, and C, respectively, where $P=(F_o^2+2F_c^2)/3$. Positions of all the hydrogen atoms were obtained on difference maps. The anisotropic and isotropic temperature factors were applied to non-hydrogen and hydrogen atoms in the final refinement. Atomic scattering factors were taken from the International Tables for Crystallography.²¹⁾ The final atomic coordinates are listed in Tables 2, 3, and 4 for A, B, and C, respectively.[#]

Results and Discussion

Crystal and Molecular Structure. Figure 1 shows the molecular structure of A with atom numbering.

Some selected bond distances and angles are listed in Table 5. The Cd atom has a formal dipositive charge. The two negative charges are supplied from two carboxylate anions of the ligands. The Cd atom in A has distorted octahedral six coordinate geometry, and bonds to four ligands. The respective ligands act as a tridentate ligand. Two of the four ligands are bonded to the Cd atom at the equatorial positions with the

[#]The tables of the anisotropic temperature factors for non-hydrogen atoms, full bond distances and angles, the parameters of hydrogen atoms, and the $F_o - F_c$ are deposited as Document No. 69028 at the Office of the Editor of Bull. Chem. Soc. Jpn.

Table 1. Crystal Data and Experimental Conditions

	A	B	C
Chemical formula	C ₈ H ₁₄ N ₄ O ₆ Cd·2H ₂ O	C ₈ H ₁₄ N ₄ OZn·2H ₂ O	C ₈ H ₁₄ N ₄ O ₆ Cd·H ₂ O
Formula weight	410.67	363.63	392.65
Crystal system	Orthorhombic	Orthorhombic	Monoclinic
Space group	<i>Pbca</i>	<i>Pbca</i>	<i>C2/c</i>
Z	4	4	4
<i>a</i> /Å	11.130(5)	11.126(3)	17.772(1)
<i>b</i> /Å	13.207(6)	12.897(2)	4.718(2)
<i>c</i> /Å	9.208(4)	8.965(1)	15.522(2)
β /°	—	—	96.648(7)
<i>V</i> /Å ³	1353.6(8)	1286.3(4)	1292.8(4)
<i>D_x</i> /Mg m ⁻³	2.015	1.878	2.017
Diffractionmeter	AFC-6S	AFC-6S	AFC-7S
Radiation	Mo <i>K</i> α	Mo <i>K</i> α	Mo <i>K</i> α
λ /Å	0.71069	0.71069	0.71073
μ (Mo <i>K</i> α)/mm ⁻¹	1.66	1.96	1.73
<i>F</i> (000)	824	752	784
Crystal dimensions/mm ³	0.40×0.30×0.30	0.40×0.30×0.30	0.40×0.30×0.30
<i>T</i> /K	296	296	296
2 θ _{max} /°	55	55	55
Range of <i>h</i> , <i>k</i> , and <i>l</i>	0≤ <i>h</i> ≤14 0≤ <i>k</i> ≤17 0≤ <i>l</i> ≤11	-14≤ <i>h</i> ≤0 0≤ <i>k</i> ≤16 0≤ <i>l</i> ≤11	-22≤ <i>h</i> ≤22 0≤ <i>k</i> ≤6 0≤ <i>l</i> ≤20
Scan technique	$\omega/2\theta$	$\omega/2\theta$	$\omega/2\theta$
Scan width/°	1.15+0.30 tan θ	1.15+0.30 tan θ	1.57+0.35 tan θ
Scan rate/° (ω) min ⁻¹	4	4	4
Independent reflections	1554	1482	1477
Observed reflections (<i>I</i> >0)	1457	1356	1373
<i>R</i> (<i>F</i>) (<i>I</i> >2σ(<i>I</i>))	0.022	0.027	0.027
<i>wR</i> (<i>F</i> ²) (<i>I</i> >0)	0.062	0.075	0.073
<i>S</i>	1.12	1.06	1.10
Extinction coefficient	0.0104(5)	—	—
(Δ/σ) _{max}	0.000	0.000	0.000
Δρ _{min} , Δρ _{max} /e Å ⁻³	-0.53, 0.55	-0.43, 0.31	-0.83, 0.34

Table 2. The Final Atomic Coordinates (×10⁴) and Equivalent Isotropic Displacement Parameters (*U*_{eq} × 10³/Å²) for A

Atoms	<i>x</i>	<i>y</i>	<i>z</i>	<i>U</i> _{eq}
Cd	0	0	0	27
O(1)	5(1)	554(1)	2432(2)	32
O(2)	-148(1)	3304(1)	4251(2)	34
O(3)	1430(1)	2788(1)	5539(2)	41
O(4)	2671(2)	1381(2)	7204(2)	50
N(1)	-1949(2)	172(1)	702(2)	28
N(2)	-1096(1)	1386(1)	4104(2)	26
C(1)	-2055(2)	947(2)	1836(2)	27
C(2)	-960(2)	938(1)	2816(2)	22
C(3)	-80(2)	1579(2)	5051(2)	26
C(4)	452(2)	2645(2)	4925(2)	26

Table 3. The Final Atomic Coordinates (×10⁴) and Equivalent Isotropic Displacement Parameters (*U*_{eq} × 10³/Å²) for B

Atoms	<i>x</i>	<i>y</i>	<i>z</i>	<i>U</i> _{eq}
Zn	0	0	0	22
O(1)	100(1)	490(1)	2300(2)	24
O(2)	-63(1)	3351(1)	4312(2)	27
O(3)	1544(1)	2806(1)	5577(2)	32
O(4)	2767(2)	1408(1)	7342(2)	40
N(1)	-1801(2)	146(1)	524(2)	21
N(2)	-957(1)	1371(1)	4040(2)	21
C(1)	-1954(2)	903(2)	1731(2)	20
C(2)	-849(2)	901(1)	2721(2)	18
C(3)	64(2)	1561(2)	4997(2)	21
C(4)	564(2)	2666(2)	4938(2)	20

nitrogen atoms of the terminal aminogroups and the oxygen atoms of the peptidegroups. The coordination of these ligands forms two five-membered chelate rings. Another two ligands are bonded to the Cd atom at the axial positions with the oxygen atoms of the terminal carboxygroups. These ligands aggregate the neighboring Cd atoms and therefore a unique three-dimensional polymer seat is formed. Since

the Cd atom is located at the crystallographic inversion center, the bonds of O(1)–Cd–O(1)ⁱ, and N(1)–Cd–N(1)ⁱ, and O(2)ⁱⁱ–Cd–O(2)ⁱⁱⁱ are linear. The conformation of the five-membered chelate ring is an envelope shape with the atom N(1) as a vertex. The torsion angles of Cd–O(1)–C(2)–C(1), N(1)–C(1)–C(2)–O(1), and Cd–N(1)–C(1)–C(2) are 5.4(2), 20.0(3), and -34.7(2)°, respectively.

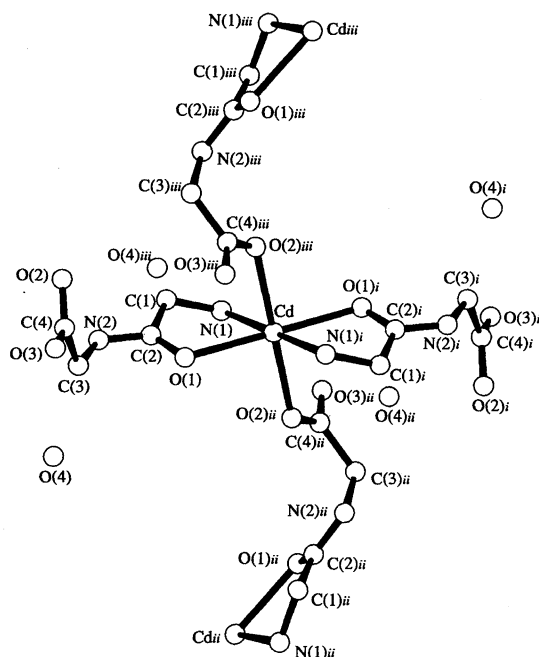


Fig. 1. Molecular structure of **A**. The italic letters indicate the symmetry related atoms. The symmetry operators are as follows: *i*: $\bar{x}, \bar{y}, \bar{z}$; *ii*: $\bar{x}, y - 1/2, \bar{z} + 1/2$; *iii*: $x, \bar{y} + 1/2, z - 1/2$.

Table 4. The Final Atomic Coordinates ($\times 10^4$) and Equivalent Isotropic Displacement Parameters ($U_{eq} \times 10^3/\text{\AA}^2$) for **C**

Atoms	<i>x</i>	<i>y</i>	<i>z</i>	U_{eq}
Cd	0	0	0	23
O(1)	-2245(2)	4181(6)	1190(2)	48
O(2)	-4078(1)	-2231(5)	743(2)	35
O(3)	-4741(1)	1493(5)	1119(1)	29
O(4)	-5000	5209(11)	2500	52
N(1)	-916(2)	1832(7)	765(2)	29
N(2)	-2749(2)	-44(6)	1477(2)	31
C(1)	-1565(2)	49(8)	858(3)	32
C(2)	-2215(2)	1579(7)	1194(2)	26
C(3)	-3454(2)	1081(9)	1716(3)	32
C(4)	-4150(2)	21(6)	1137(2)	24

The bond length of Cd–N(1) is significantly shorter than the van der Waals distance of Cd–N(bipyridine), 2.389 Å.²²⁾ This means that the nitrogen atom of the terminal amino-group of the dipeptide is strongly bonded to the Cd atom. Although the oxygen atom of the peptide-group is bonded to the Cd atom, the bond length of the peptide C(2)–N(2) is close to that of the metal-free glycylglycine molecule, 1.3333(5) Å.²³⁾ This indicates that the electron delocalization does not extend over the peptide moiety. The bond length of C(4)–O(2) is significantly longer than the alternate carboxy C(4)–O(3) distance. This is due to the result of the electron delocalization between the C(4)–O(2) and the Cd atom for bonding.

Figure 2 shows the crystal structure of **A** viewed along the *c*-axis. The seats of polymers are aligned perpendicular

Table 5. Selected Bond Lengths (Å) and Angles (°) for **A**

Cd–O(1)	2.356(2)	O(1)–Cd–O(1) ^{<i>i</i>}	180
Cd–O(2)	2.349(2)	O(1)–Cd–O(2) ^{<i>ii</i>}	90.96(6)
Cd–N(1)	2.275(2)	O(1)–Cd–O(2) ^{<i>iii</i>}	89.04(6)
O(1)–C(2)	1.239(2)	O(1)–Cd–N(1)	72.61(5)
O(2)–C(4)	1.261(3)	O(1)–Cd–N(1) ^{<i>i</i>}	107.39(5)
O(3)–C(4)	1.240(2)	O(2) ^{<i>ii</i>} –Cd–O(2) ^{<i>iii</i>}	180
N(1)–C(1)	1.466(2)	O(2) ^{<i>ii</i>} –Cd–N(1)	94.52(6)
N(2)–C(2)	1.334(2)	O(2) ^{<i>iii</i>} –Cd–N(1)	85.48(6)
N(2)–C(3)	1.450(2)	N(1)–Cd–N(1) ^{<i>i</i>}	180
C(1)–C(2)	1.516(2)	Cd–O(1)–C(2)	113.3 (1)
C(3)–C(4)	1.532(3)	Cd–N(1)–C(1)	110.4 (1)
		O(1)–C(2)–C(1)	122.0 (2)
		N(1)–C(1)–C(2)	110.7 (2)

i: $\bar{x}, \bar{y}, \bar{z}$; *ii*: $\bar{x}, y - 1/2, \bar{z} + 1/2$; *iii*: $x, \bar{y} + 1/2, \bar{z} - 1/2$.

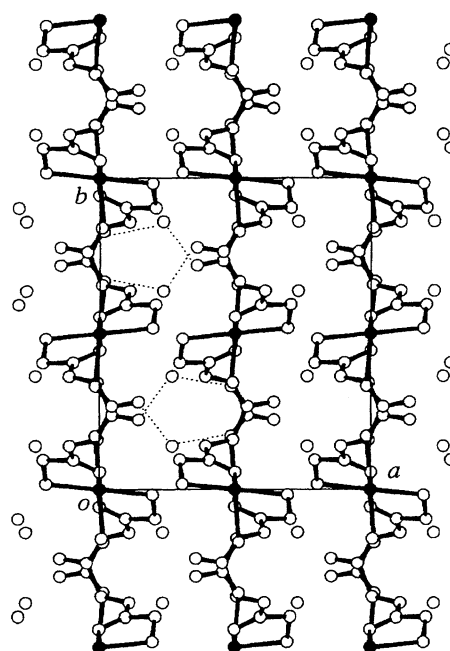


Fig. 2. Crystal structure of **A** viewed along the *c*-axis. Broken lines indicates the hydrogen bonds.

to the *a*-axis. The water molecules are located between the seats, and are hydrogen bonded to the oxygen atoms of the terminal carboxygroups, through O(4)–H(4A)···O(2) and O(4)–H(4B)···O(3). The distances and angles are as follows: O(4)···O(2); 2.803(3) Å, H(4A)···O(2); 1.95(4) Å, O(4)–H(4A)···O(2); 169(3)°, O(4)···O(3); 2.777(2) Å, H(4B)···O(3); 1.94(4) Å, and O(4)–H(4B)···O(3); 161(3)°.

Figure 3 shows the molecular structure of **B** with atom numbering.

Some selected bond distances and angles are listed in Table 6. Since the crystal of **B** is isomorphous to the crystal of **A**, the geometry and the conformation of **B** are almost the same as that of **A**. The corresponding torsion angles of the five-membered chelate ring are as follows: Zn–O(1)–C(2)–C(1); 7.1(2), N(1)–C(1)–C(2)–O(1); 15.3(3), and Zn–N(1)–C(1)–C(2); –29.9(2)°. The bond lengths between the

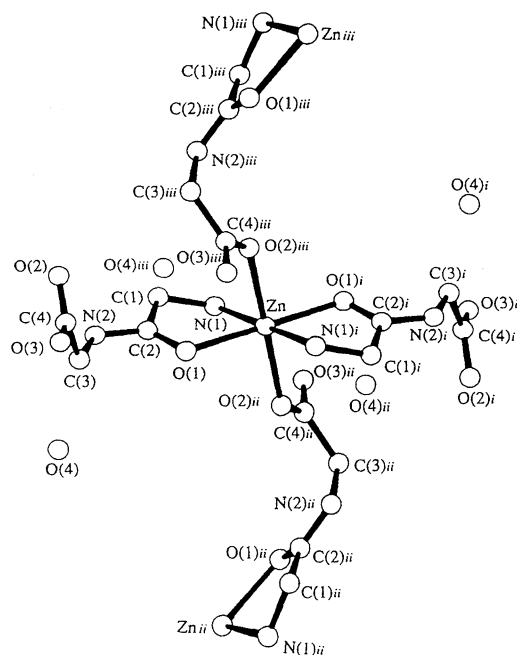


Fig. 3. Molecular structure of **B**. The italic letters indicate the symmetry related atoms. The symmetry operators are as follows: *i*: $\bar{x}, \bar{y}, \bar{z}$; *ii*: $\bar{x}, y-1/2, \bar{z}+1/2$; *iii*: $x, \bar{y}+1/2, z-1/2$.

Table 6. Selected Bond Lengths (Å) and Angles (°) for **B**

Zn–O(1)	2.159(2)	O(1)–Zn–O(1) ^{<i>i</i>}	180
Zn–O(2)	2.215(1)	O(1)–Zn–O(2) ^{<i>ii</i>}	90.77(6)
Zn–N(1)	2.067(2)	O(1)–Zn–O(2) ^{<i>iii</i>}	89.23(6)
O(1)–C(2)	1.241(2)	O(1)–Zn–N(1)	78.84(6)
O(2)–C(4)	1.258(3)	O(1)–Zn–N(1) ^{<i>i</i>}	101.16(6)
O(3)–C(4)	1.245(2)	O(2) ^{<i>ii</i>} –Zn–O(2) ^{<i>iii</i>}	180
N(1)–C(1)	1.467(3)	O(2) ^{<i>ii</i>} –Zn–N(1)	93.15(6)
N(2)–C(2)	1.334(2)	O(2) ^{<i>iii</i>} –Zn–N(1)	86.85(6)
N(2)–C(3)	1.444(2)	N(1)–Zn–N(1) ^{<i>i</i>}	180
C(1)–C(2)	1.516(3)	Zn–O(1)–C(2)	111.8 (1)
C(3)–C(4)	1.531(3)	Zn–N(1)–C(1)	109.9 (1)
		O(1)–C(2)–C(1)	120.8 (2)
		N(1)–C(1)–C(2)	109.7 (2)

i: $\bar{x}, \bar{y}, \bar{z}$; *ii*: $\bar{x}, y-1/2, \bar{z}+1/2$; *iii*: $x, \bar{y}+1/2, z-1/2$.

metal and the coordinated atoms are shorter than those of **A**. Such shortening of the bond lengths is due to the difference of the ionic radii between Zn and Cd, the values are 1.332 and 1.489 Å for Zn and Cd atoms, respectively.²⁴⁾

The crystal structure of **B** is also the same as that of **A**. The corresponding distances and angles of the intermolecular hydrogen bonds between the water molecules and the oxygen atoms of the terminal carboxygroup are as follows: O(4)···O(2); 2.850(2) Å, H(4A)···O(2); 2.09(4) Å, O(4)–H(4A)···O(2); 171(3)°, O(4)···O(3); 2.759(2) Å, H(4B)···O(3); 1.83(4) Å, and O(4)–H(4B)···O(3); 162(3)°.

Above all, **B** is structurally similar to **A** having the same ligand. This indicates that the Cd nucleus is better suited for probing the Zn nucleus.

Figure 4 shows the molecular structure of **C** with atom

Table 7. Selected Bond Lengths (Å) and Angles (°) for **C**

Cd–O(2)	2.299(2)	O(2) ^{<i>ii</i>} –Cd–O(2) ^{<i>iii</i>}	180
Cd–O(3)	2.405(2)	O(2) ^{<i>ii</i>} –Cd–O(3) ^{<i>v</i>}	92.12(9)
Cd–N(1)	2.291(3)	O(2) ^{<i>iii</i>} –Cd–O(3) ^{<i>v</i>}	87.88(9)
O(1)–C(2)	1.229(4)	O(2) ^{<i>ii</i>} –Cd–N(1)	91.9 (1)
O(2)–C(4)	1.240(4)	O(2) ^{<i>iii</i>} –Cd–N(1)	88.1 (1)
O(3)–C(4)	1.257(4)	O(3) ^{<i>iv</i>} –Cd–O(3) ^{<i>v</i>}	180
N(1)–C(1)	1.449(4)	O(3) ^{<i>iv</i>} –Cd–N(1)	88.5 (1)
N(2)–C(2)	1.332(4)	O(3) ^{<i>v</i>} –Cd–N(1)	91.5 (1)
N(2)–C(3)	1.449(4)	N(1)–Cd–N(1) ^{<i>i</i>}	180
C(1)–C(2)	1.507(5)	N(1)–C(1)–C(2)	114.1 (3)
C(3)–C(4)	1.526(5)	N(2)–C(2)–C(1)	116.3 (3)
		N(2)–C(3)–C(4)	113.3 (3)

i: $\bar{x}, \bar{y}, \bar{z}$; *ii*: $x+1/2, y+1/2, z$; *iii*: $\bar{x}-1/2, \bar{y}-1/2, \bar{z}$; *iv*: $x+1/2, y-1/2, z$; *v*: $\bar{x}-1/2, \bar{y}+1/2, \bar{z}$.

numbering.

Some selected bond distances and angles are listed in Table 7. The formal charge of the Cd atom is +2. The two negative charges are supplied from two carboxylate anions of the ligands. Although the ligand and the central metal atom are the same as in **A**, the molecular structure of **C** is quite different from that of **A**. The Cd atom in **C** has regular octahedral six coordinate geometry, and bonds to four oxygen atoms of the terminal carboxygroup and two nitrogen atoms of the terminal aminogroup from six ligands. In this case, the ligand also acts as a tridentate ligand. The three coordination atoms are bonded to three different Cd atoms. Two oxygen atoms of the terminal carboxygroup bind two neighboring Cd atoms, and the nitrogen atom of the terminal aminogroup bonds to another Cd atom. As a consequence of this coordination, a unique three-dimensional polymer seat is formed. Since the oxygen atom of the peptide is free from the coordination, the five-membered chelate ring is not formed between the terminal aminogroup and the adjacent oxygen atom of the peptide. It may be expected that the NMR chemical shift of C(4) (terminal carboxy) will be slightly different from that of C(2) (peptide carbonyl) in the complex, as is shown by ¹³C CP/MAS NMR spectroscopy of **C**. Since the Cd atom is located in the crystallographic inversion center, the bonds of O(2)^{*ii*}–Cd–O(2)^{*iii*}, O(3)^{*iv*}–Cd–O(3)^{*v*}, and N(1)–Cd–N(1)^{*i*} are linear. The most interesting result in the molecular structure of **C** is the difference of the bond length between the Cd atom and the oxygen atoms of the terminal carboxy-group. The bond length of Cd–O(3) is considerably longer than that of Cd–O(2). This difference may be caused by the formation of a hydrogen bond between O(3) and a water molecule. This is to say, O(2) would be strongly bonded to Cd and O(3) weakly bonded.

Figure 5 shows the crystal structure of **C** viewed along the *b*-axis. The seats of polymers are aligned perpendicular to the *c*-axis. The water molecules are located between the seats, and are hydrogen-bonded to the oxygen atoms of the terminal carboxygroups, through O(4)–H(4)···O(3). The distances and angles of O(4)···O(3), H(4)···O(3), and O(4)–H(4)···O(3) are 2.848(4) Å, 2.06(6) Å, and 161(7)°,

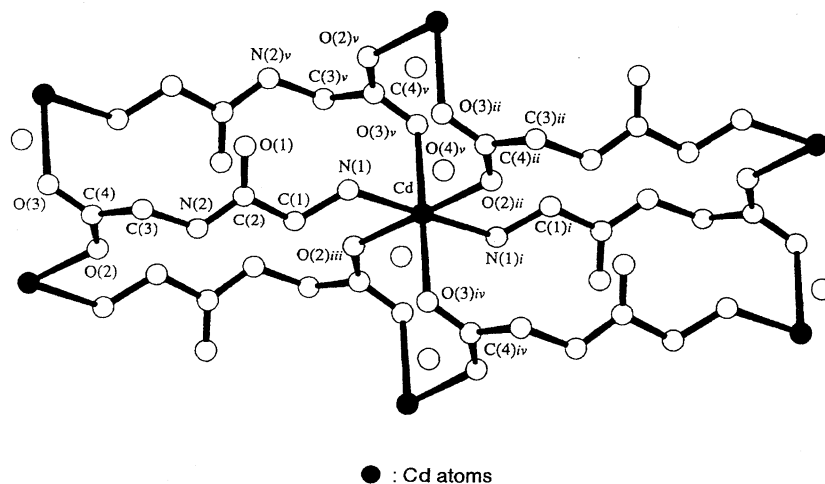


Fig. 4. Molecular structure of **C**. The italic letters indicate the symmetry related atoms. The symmetry operators are as follows: *i*: $\bar{x}, \bar{y}, \bar{z}$; *ii*: $x+1/2, y+1/2, z$; *iii*: $\bar{x}-1/2, \bar{y}-1/2, \bar{z}$; *iv*: $x+1/2, y-1/2, z$; *v*: $\bar{x}-1/2, \bar{y}+1/2, z$.

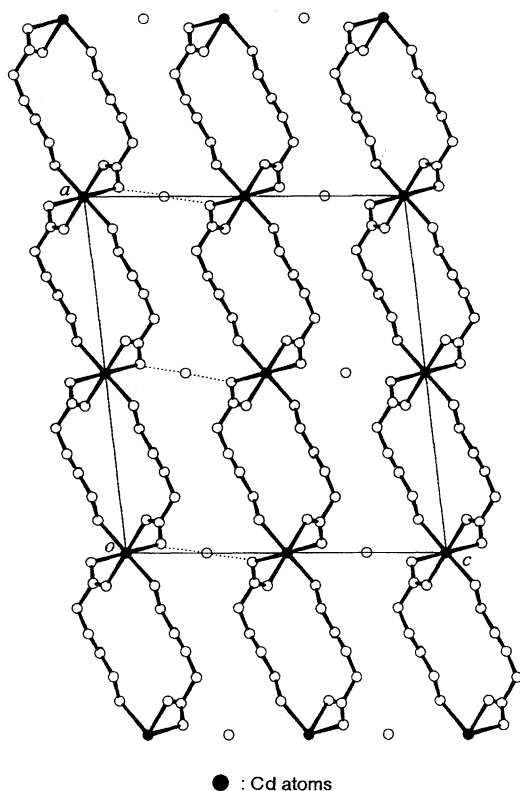


Fig. 5. Crystal structure of **C** viewed along the *b*-axis. Broken lines indicates the hydrogen bonds.

respectively.

There is a strong presumption that the crystal structure of the bis(glycylglycinato)zinc(II) complex prepared to adjust the pH to 9, is the same as **C** considering the argument of Tyzebiatowska et al.²⁵⁾

Further structural details are discussed below in the context of correlations with the ^{113}Cd and ^{13}C solid state NMR spectra.

^{113}Cd CP/MAS NMR Spectra. The ^{113}Cd CP/MAS

NMR spectra of **A** and **C** are shown in Fig. 6. Many sharp, intense peaks appear over a wide range. The spectra consist of a series of peaks separated by the spinning frequency (spinning side bands). These are cases of "slow spinning", in which the MAS frequency is considerably less than the shift anisotropy. The peak that is independent of the spinning frequency corresponds to the isotropic chemical shift. The isotropic peaks obtained from Fig. 6 were **A**: $\delta = 169.3$ and **C**: $\delta = 91.5$. The signal of **C** shows an upfield chemical shift ($\Delta\delta = 77.8$) compared with the peak for **A**. From the results of X-ray structural analysis, the Cd atom of **A** is six coordinate, two five-membered chelate rings are formed between the terminal aminogroups, and the adjacent oxygens (peptide), and the bonds lie as a distorted octahedral. For **C**, the six coordinate Cd atom is bonded to the four terminal carboxy-groups and the two terminal aminogroups of the peptide ligands, a five-membered chelate ring is not formed, and the bond has regular octahedral coordination geometry.

As a general trend for the ^{113}Cd chemical shift,¹⁵⁾ 1) a Cd atom bonded to a nitrogen atom seems to decrease shielding (low field shift), 2) one bonded to an oxygen atom increases shielding (high field shift), and 3) one forming a chelate ring seems to decrease shielding. Above all, it is reasonable the ^{113}Cd chemical shift of **A** ($\delta = 169.3$) is at a lower field than **C** ($\delta = 91.5$). In order to obtain further information about the distortion from an octahedral symmetry, we noted the patterns of spinning side bands for the ^{113}Cd spectra of **A** and **C**. It is interesting that apparent distortions in the octahedral symmetry are sufficient to produce large chemical shift anisotropies.²⁶⁾ The intensity pattern of the spinning side bands in Fig. 6 reflects the chemical shift anisotropy obtained in a nonspinning experiment. As shown in Fig. 6, the cadmium ion in **A** showing many spinning side bands produces large chemical shift anisotropy, so the cadmium ion is located apparently within a distortion of the octahedral symmetry. On the other hand, with **C** showing much fewer spinning side bands, the Cd produces small chemical shift anisotropy, so the cadmium ion is located in the directions

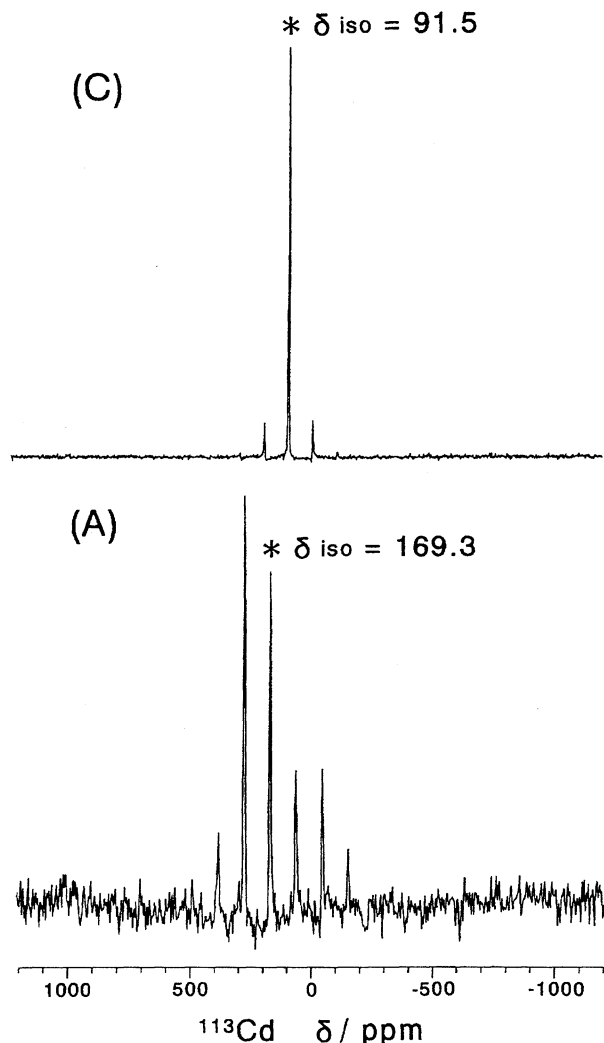


Fig. 6. ^{113}Cd CP/MAS NMR spectra of A[$\text{Cd}(\text{glygly})_2 \cdot 2\text{H}_2\text{O}$ pH=6] spinning at 5683 Hz (below) and C[$\text{Cd}(\text{glygly})_2 \cdot \text{H}_2\text{O}$ pH=9] spinning at 5716 Hz (above). The chemical shift scale is in δ relative to $\text{Cd}(\text{ClO}_4)_2 \cdot 6\text{H}_2\text{O}$. The isotropic peak that is independent of the spinning frequency corresponds to the isotropic chemical shift.

required for octahedral coordination.

^{13}C CP/MAS NMR Spectra. Figure 7 shows the ^{13}C CP/MAS NMR spectra of A, B, and C. First, the solid state ^{13}C NMR spectra of A and B were studied in order to find out the structural consistency between Cd and Zn complexes. In the spectra of A and B, methylene carbon peaks (1) appear at $\delta = 42.6$ and 42.5 , respectively. Such coinciding of the chemical shifts of the methylene carbons means that the terminal amine and terminal carboxy oxygen of the dipeptide bond to the Cd nucleus. The peaks for carbonyl carbon (peptide) (2) and terminal carboxyl carbon (3) of A and B overlap and the chemical shifts show at $\delta = 175.8$ and 175.6 , respectively. This means that the carbonyl oxygen (peptide) and terminal carboxyl group of the dipeptide each bond to the Cd nucleus. After all, the chemical shifts of all peaks were almost similar in A and B. This suggests that the A and B complexes have the same molecular structure in one unit cell and the bonding

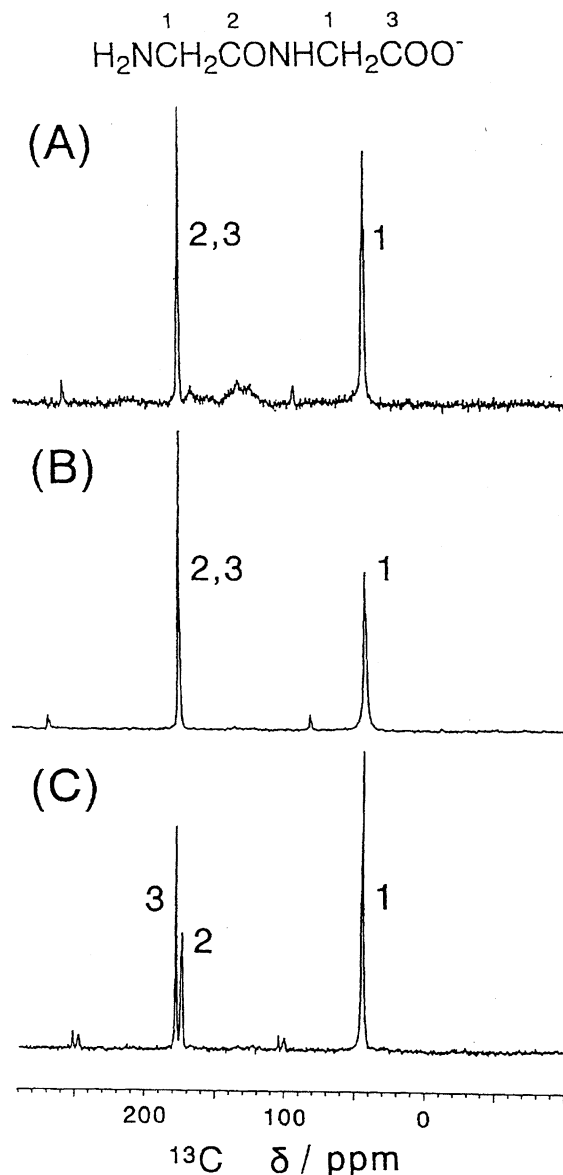


Fig. 7. ^{13}C CP/MAS NMR spectra of the powdered crystal complexes A, B, and C.

around the Cd or Zn nucleus consists of the terminal aminogroups, the adjacent carbonyl oxygens (peptide), and the terminal carboxygroups from other dipeptide ligands. On the other hand, the spectrum of C shows three ^{13}C peaks at $\delta = 43.7$, 173.5 , and 177.4 , corresponding to the chemical shifts for the methylene carbon peak (1), the nonbonding carbonyl carbon peak (2), and the terminal carboxyl carbon peak (3) of the dipeptide ligand, respectively. The chemical shift of the nonbonding carbonyl carbon (2) was determined to be at $\delta = 173.5$, because the ^{13}C NMR chemical shift of the carbonyl carbon (peptide) for solid glycylglycine ($2\text{H}_2\text{O}$) is $\delta = 173.3$.

Above all, it can be said that the ^{113}Cd and ^{13}C CP/MAS NMR experiments provided very useful information in the structural analysis of Cd-dipeptide complexes in the solid state.

In conclusion, **A**, prepared to adjust the pH to 6 from Cd-(NO₃)₂ and glycylglycine has a five-membered chelate ring formed between the terminal amino-group and the adjacent peptide oxygen. On the other hand, **C**, prepared to adjust the pH to 9, does not form a five-membered chelate ring.

References

- 1) B. L. O' Dell and B. J. Campbell, "Comprehensive Biochemistry," ed by M. Florkin and E. H. Stotz, Elsevier Pub. Co., Amsterdam (1970), Vol. 21, p. 179.
- 2) J. E. Coleman and B. L. Vallee, *J. Biol. Chem.*, **235**, 390 (1960); **237**, 3430 (1962); *Biochem.*, **1**, 1083 (1962).
- 3) M. J. A. Rainer and B. M. Rode, *Inorg. Chim. Acta*, **58**, 59 (1982).
- 4) M. M. Probst and B. M. Rode, *Inorg. Chim. Acta*, **92**, 75 (1984).
- 5) D. L. Rabenstein and S. Libich, *Inorg. Chem.*, **11**, 2960 (1972).
- 6) M. J. B. Ackerman and J. J. H. Ackerman, *J. Phys. Chem.*, **84**, 3151 (1980).
- 7) C. F. Jensen, S. Deshmukh, H. J. Jakobsen, R. R. Inners, and P. D. Ellis, *J. Am. Chem. Soc.*, **103**, 3659 (1981).
- 8) H. J. Jakobsen and P. D. Ellis, *J. Phys. Chem.*, **85**, 3367 (1981).
- 9) M. Munakata, S. Kitagawa, and F. Yagi, *Inorg. Chem.*, **25**, 964 (1986).
- 10) S. M. Wang and R. Gilpin, *Anal. Chem.*, **55**, 493 (1983).
- 11) R. J. Frook, H. C. Freeman, C. J. Moore, and M. L. Scudder, *J. Chem. Soc., Chem. Commun.*, **1973**, 753.
- 12) M. Mehring, "High Resolution NMR Spectroscopy in Solids," Springer-Verlag, New York (1976), p.107.
- 13) J. Schaefer and E. O. Stejskal, "Topics in C-13 NMR Spectroscopy," ed by G. C. Levy, Wiley, New York (1979), Chap. 4.
- 14) L. E. D'iaz, F. Morin, C. L. Mayne, D. M. Grant, and C. Chang, *Magn. Reson. Chem.*, **24**, 167 (1986).
- 15) P. G. Mennitt, M. P. Shatlock, V. J. Bartuska, and G. E. Maciel, *J. Phys. Chem.*, **85**, 2087 (1981).
- 16) P. D. Ellis, R. R. Inners, and H. J. Jakobsen, *J. Phys. Chem.*, **86**, 1506 (1982).
- 17) S. Nishikiori, C. I. Ratcliffe, and J. A. Ripmeester, *Can. J. Chem.*, **68**, 2270 (1990).
- 18) S. Lacelle, W. C. Stevens, D. M. Kurtz, Jr., J. W. Richardson, Jr., and R. A. Jacobson, *Inorg. Chem.*, **23**, 930 (1984).
- 19) G. Cascarano, C. Giacovazzo, A. Guagliardi, M. C. Burla, G. Polidori, and M. Camalli, *J. Appl. Crystallogr.*, **27**, 435 (1994).
- 20) G. M. Sheldrick, "SHELXL-93," Program for the Refinement of the Crystal Structure, University of Gottingen, Germany (1993).
- 21) "International Tables for Crystallography," ed by A. J. C. Wilson, Kluwer Academic Publisher, Dordrecht (1992), Vol. C, Tables 6.1.1.4 (pp. 500—502), 4.2.6.8 (pp. 219—222), and 4.2.4.2 (pp. 193—199).
- 22) P. F. Rodesiler, R. W. Turner, N. G. Charles, E. A. H. Griffith, and E. L. Amma, *Inorg. Chem.*, **23**, 999 (1984).
- 23) A. Kvick, A. R. Al-Karaghoul, and T. F. Koetzle, *Acta Crystallogr., Sect. B*, **B33**, 3796 (1977).
- 24) N. A. Lange, "Lange's Hand Book of Chemistry," ed by J. A. Dean, McGraw-Hill, New York (1973).
- 25) B. J. Tyzebiatowska, L. L. Grazynski, and H. Kozlowski, *J. Inorg. Nucl. Chem.*, **39**, 1269 (1977).
- 26) R. S. Honkonen, P. S. Marchetti, and P. D. Ellis, *J. Am. Chem. Soc.*, **108**, 912 (1986).